Journal of Applied Polymer Science

Cellulose nanofibers from the skin of beavertail cactus, *Opuntia Basilaris*, as reinforcements for polyvinyl alcohol

Adel Ramezani Kakroodi,[1] Suhara Panthapulakkal,[1] Mohini Sain,[1,2] Abdullah Asiri[3]

[1]Centre for Biocomposites and Biomaterials Processing, Faculty of Forestry, University of Toronto, Toronto, Canada
[2]Adjunct, Centre of Advanced Chemistry, King Abdulaziz University, Jeddah, Saudi Arabia
[3]Centre of Advanced Chemistry, King Abdulaziz University, Jeddah, Saudi Arabia
Correspondence to: A. Ramezani Kakroodi (E-mail: adel.ramezanikakroodi@utoronto.ca)

ABSTRACT: In this study, the skin of the beavertail cactus, *Opuntia Basilaris*, was used for the isolation of cellulose nanofibers using a chemo-mechanical technique. It was shown that the skins had a relatively high cellulose content, whereas their lignin content was low. Fourier transform infrared spectroscopy and X-ray diffraction proved that the isolation of cellulose nanofibers from the amorphous components of the skins was performed successfully. The cactus skins were also shown to have a high content of calcium oxalate crystals. Morphological observations proved that the isolated cellulose fibers had diameters in the range of 10–50 nm. It was shown that the addition of nanofibers increased the modulus and strength of the polyvinyl alcohol matrix significantly, whereas the elongation at break decreased. Thermogravimetric analysis proved that: (i) isolated nanofibers had higher thermal stabilities than the cactus skins, and (ii) inclusion of nanofibers increased the stability of polyvinyl alcohol noticeably. © 2015 Wiley Periodicals, Inc. J. Appl. Polym. Sci. **2015**, *132*, 42499.

KEYWORDS: composites; cellulose and other wood product; mechanical properties; morphology

Received 8 December 2014; accepted 13 May 2015
DOI: 10.1002/app.42499

INTRODUCTION

Cellulose, in the form of nanofibers, is the main building unit for wood and other natural fibers and the most abundant naturally made polymer. Cellulose nanofibers are present in plant cell walls in the form of fiber bundles along with other polymers such as lignin.[1–4] Thus, extraction of cellulose nanofibers usually consists of isolation of the fibers from other constituents of the plants followed by separation of individual fibers, usually using mechanical treatments. Several isolation techniques have already been developed, including mechanical methods, chemo-mechanical methods, and enzymatic methods.[2] Among these, the chemo-mechanical method has been more common due to lower energy consumption and convenience.[5] In chemo-mechanical method, the cellulose fibers are isolated from lignin, pectin, protein, hemicellulose, and waxes using several chemical treatments. These treatments are then followed by mechanical grinding for creation of individual fibers.

During the past decades, cellulose nanofibers have been extracted from a variety of plants, including wood, kenaf, flax, soybean, wheat straw, etc., and used as reinforcements for several polymers.[6–12] The produced composites are of great interest in automotive and construction industries and in production of novel mobile electronics. Successful inclusion of cellulose nanofibers into polymers is expected to increase their mechanical properties substantially due to (i) high mechanical properties of these nanofibers (tensile modulus of as high as 134 GPa for cellulose crystals and tensile strengths of up to 10 GPa),[13] (ii) large specific surface area and aspect ratios of the produced nanofibers, and (iii) creation of a web-like network between the nanofibers at high concentrations of the fibers.[14] Such networks are created because of the flexible structure of cellulose nanofibers, leading to the mechanical interlocking of the fibers, and also due to creation of hydrogen bonds between the fibers.

However, previous investigations [2,7] have proven that the addition of cellulose nanofibers to polymers usually causes only moderate improvements in their mechanical properties. Severe agglomeration of nanofibers, because of the creation of strong hydrogen bonds between them, is the major contributor for such behavior.[2,7] Agglomeration of the nanofibers results in a number of consequences such as increase in diameter and reduction in aspect ratio and specific active surface area of the reinforcing phase. As a result, cellulose nanofibers are usually kept in the form of dilute aqueous suspensions and their composites are prepared by solution casting technique using water-soluble polymers such as polyvinyl alcohol (PVA).

Beavertail cactus, *Opuntia Basilaris,* is a species of Cactaceae family, which is widespread in the arid areas of southwestern United States.[15] Production of high-performance cellulose nanofibers from this plant would provide a novel and abundant resource for bio-based, strong, and light weight composites. As a result, this study has been devoted to the isolation of cellulose nanofibers from the skin of beavertail cactus plant using a chemo-mechanical technique. The isolated nanofibers were used for the production of high-strength nanofibrous films and reinforcement of PVA matrix using solvent casting technique. Composites with different concentrations of cellulose nanofibers (2, 5, 7, and 10% by weight) were prepared. A comprehensive characterization was performed on the properties of the cactus skin, isolated cellulose nanofibers, and PVA/nanocellulose composites.

MATERIALS AND METHODS

Materials

Opuntia Basilaris plants were purchased from Sheridan Nurseries, Toronto, Canada. Polyvinyl alcohol, Elvanol 71-30 from DuPont, was used as matrix in all composites. Reagent grade chemicals for the chemical treatment of the cactus skins were used as received.

Chemical Composition of Cactus Skin

Extractive content of the cactus skin in the form of dried powder, 40 mesh, was quantified using ASTM D1105-96 standard. A three-step extraction process was used: (i) extraction of powder using a solution of two parts of toluene to one part of 95% ethanol, (ii) extraction using 95% ethanol, and (iii) extraction using boiled distilled water. The extractive-free sample was then oven dried at 105°C over night and weighed. The following formula was used for the calculation of extractives content in the skins:

$$Extractives\ (\%) = \frac{w_b - w_a}{w_b} \times 100 \quad (1)$$

where w_b and w_a are the weight of dried powder before and after the extractions, respectively.

Chemical compositions (α-cellulose, hemicellulose, and lignin) of the extractive-free cactus skin powder were analyzed using the procedure proposed by Zobel *et al.*[16] and technical association of the pulp and paper industry (TAPPI) standard. Ash content of the powder was also measured by heating a sample at 575°C in a muffle furnace for 4 h. All of the above characterizations were performed on three samples to provide an average and standard deviation.

Isolation of Nanofibers and Preparation of Nanofibrous Films

The skins, with thicknesses of 3–4 mm, were removed using a knife and washed with hot water. The skins were then oven dried at 80°C over night and then ground to prepare powder with average size of 2 mm.

Cellulose nanofibers were isolated from the skin using a chemo-mechanical technique. First, the skin powder was treated with a 0.05*N* HCl solution, Caledon Laboratories, at 70°C for 2 h in a water bath. The pH of the system was subsequently adjusted to 9.5 using ammonium hydroxide, from J.T. Baker. The mixture was kept overnight at 4°C to remove fat and pectin. At this stage, the sample was washed with distilled water and then air dried. Then, the sample was treated with 4% sodium hydroxide solution, Caledon Laboratories, at 70°C for 2 h, whereas the sample to NaOH solution ratio was 1 : 10 (wt./wt.). Bleaching of the skin powder was performed using an acidified sodium chlorite method to remove lignin. Around 100 g of the skin powder was added to a solution of 800 mL of distilled water, 8.6 mL of glacial acetic acid, Caledon Laboratories, and 9 g of sodium chlorite, Alfa Aesar, and the system was kept in a water bath at 70°C. Nine grams of sodium chlorite was added again after the first and second hours. The system was kept in the water bath for 2 more hours, 4 h in total, with frequent stirring. After the bleaching process, the mixture was cooled down to room temperature and filtered under vacuum and carefully washed with distilled water.

Mechanical defibrillation of the purified cellulose fibers was performed using a Masuko commercial grinder at 1500 rpm for 12 min. Eventually, a uniform suspension of cellulose nanofibers in water with concentration of 0.17 wt % was produced.

Preparation of Nanofibrous Films and PVA/Cellulose Nanocomposites

Nanofibrous films with an average thickness of 50 μm were prepared by filtration of the homogenous suspension of nanofibers using a membrane filter under suction. The filtered film was then pressed between the membranes at room temperature, 23°C, under 345 kPa for 15 min and dried overnight at 60°C.

PVA-based nanocomposites were produced using a solution casting method. PVA powder was first dissolved in hot, 80°C, distilled water for 1 h by continuous stirring. Different amounts of the cellulose nanofiber suspension were then added to the solution to produce composites with 2, 5, 7, and 10 wt % of nanofibers and the stirring was continued for 1 more hour. Then, ultrasonication of the mixtures was performed for 1 h at room temperature for further dispersion of nanofibers and removal of possible air bubbles. The mixtures were cast in Petri dishes and left to dry at room temperature for 168 h followed by drying in oven at 50°C for 24 h. Transparent and flexible nanofiber-reinforced films with average thickness of 130 μm were obtained. The nanocomposites were coded according to their fiber contents on a weight basis. For instance, PVA/NC(5) denotes composite film with 5% nanocellulose in PVA matrix.

Characterizations

Fourier transform infrared (FTIR) spectrum of the untreated cactus skin powder and the isolated cellulose nanofiber powder were examined using a Bruker Tensor 27 FTIR spectrometer, Bruker Optic. The powders were first mixed with KBr with a powder to KBr weight ratio of 1 : 100. The mixture was then pressed and a thin and transparent pellet was obtained.

X-ray diffraction (XRD) patterns of untreated cactus skin powder and the prepared cellulose nanofiber powder were determined using a Philip PW3710 X-ray Diffractometer using a Cu-Kα radiation, $\lambda = 1.5406$ Å, with a voltage of 40 kV and a current of 40 mA with a scan angle from 5° to 40° and a scan speed of 0.008 (2θ/s). The radiation was Ni filtered. The cellulose nanofiber was prepared by drying the nanofiber suspension overnight at

Table I. Chemical Composition of the Cactus Skins

	Extractive Content (%)	Composition of Extractive-free Cactus Skin (%)				
		α-Cellulose	Hemicellulose	Klason Lignin	Soluble Lignin	Ash
Cactus skin	23.3 ± 1.8	33.72 ± 2.80	21.48 ± 3.14	4.47 ± 0.51	3.03 ± 0.45	26.25 ± 3.92

105°C and crushing the remains with a mortar and pestle. A mat of the powdered fibers was prepared and reflection mode was used. Crystallinity index (CI) was used to determine the relative amount of crystalline phase and was defined as the ratio of weight of crystalline cellulose to the total weight of the sample. XRD peak height method[17] was used for calculation of CI as follows:

$$CI = \frac{H_{002} - H_m}{H_{002}} \quad (2)$$

where H_{002} is the height of the 002 peak ($2\theta = 21.6°$), H_m is the height of the minimum ($2\theta = 17.8°$) between the 002 peak and the 101 peak ($2\theta = 15.5°$).

Morphological analysis of the produced cellulose nanofibers was performed by transmission electron microscopy (TEM) using a Hitachi H-7000 TEM (Hitachi, Japan) at a voltage of 75 kv. Scanning electron microscopy (SEM) was also used to study the morphology of the PVA-based nanocomposites. Composites with different concentrations of cellulose nanofiber from cactus skin were cryogenically fractured, in liquid nitrogen, and were coated with gold. Then, a Quanta FEG 250 scanning electron microscope was used to take the micrographs from the cross-sections at a voltage of 10 kV.

Tensile properties of the nanofibrous film and the PVA-based nanocomposites were measured according to ASTM D638, type V. Tension tests were performed at a crosshead speed of 1 mm/min on an Instron model 3367 with a 2-kN load cell at room temperature (23°C). All samples were oven-dried for 1 h at 105°C and kept in a desiccator before testing. The data reported are tensile modulus, tensile strength, and tensile elongation at break. Each composition was tested with a minimum of five specimens to extract an average and standard deviation for each property.

Thermal stabilities of untreated cactus skin, extracted nanofibers, and the nanocomposites were investigated using a TGA Q500 (TA Instruments) at a heating rate of 10°C/min from 50 to 600°C. The tests were performed under nitrogen atmosphere.

To measure the density of composites, the volumes (cm^3) and masses (g) of rectangular films, with average thickness of 130 μm, were carefully measured and the ratio of mass/volume was reported. For each compound, a minimum of five specimens were used to extract an average and standard deviation for densities of the films.

RESULTS AND DISCUSSIONS

Chemical Composition of Cactus Skin

Table I presents the extractive content and chemical composition of the extractive free cactus skins. It is shown in Table I that cactus skins had a relatively high cellulose content, whereas their lignin contents were low. This combination suggests that the cactus skins are a suitable resource for the isolation of cellulose nanofibers. The ash content of cactus skin was 26.25%, which is much higher than the values of ash contents for other plants, such as kenaf, 3.0%,[18] and Aloe vera rinds,8.89%,[17] reported in the literature.

FTIR Spectroscopy

FTIR spectroscopy is a useful tool for the determination of changes in the chemical composition of cactus skins, such as removal of lignin and hemicellulose and change in the concentration of cellulose, after the chemo-mechanical modifications. Figure 1 presents the FTIR spectra between the wave numbers of 1800–800 cm^{-1} to facilitate the observations. The peak at 1737 cm^{-1} in the untreated cactus skin powder can be ascribed to the acetyl or uronic ester groups from hemicellulose or to the carboxylic group of the ferulic and *p*-coumeric acids from lignin or possibly hemicellulose. Figure 1 shows that the intensity of this peak has been substantially reduced after the chemical treatment of the skins, which signals separation of lignin and hemicellulose. The figure also shows that the peak at 896 cm^{-1} is much more prominent in case of the chemically treated skins.[7] This peak is attributed to a typical structure of cellulose and proves that the isolation of cellulose has been performed successfully. Two prominent peaks at 1630 and 1325 cm^{-1} are ascribed to the stretching vibrations of the carboxylate groups of inorganic components, calcium oxalate crystals, of the cactus skins. It has been reported that cacti plants often have high contents of calcium oxalate crystals, for instance as much as 85% of dry mass in *Cactus senilis*.[19]

XRD, Crystallinity Measurements, and Degree of Polymerization

Creation of hydrogen bonds between cellulose fibers is known to produce a generally ordered system with high crystallinity.

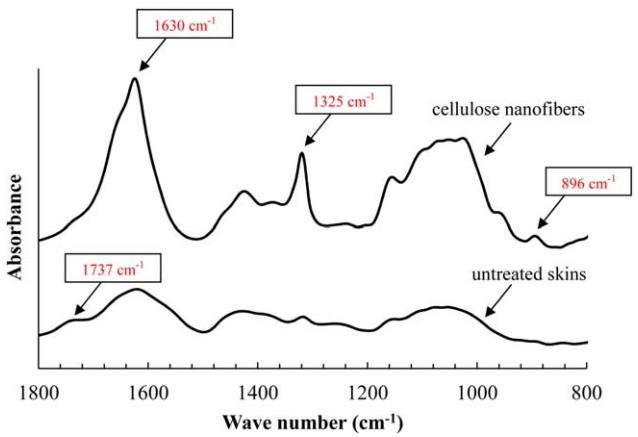

Figure 1. FTIR spectra of untreated cactus skins and the isolated cellulose nanofibers. [Color figure can be viewed in the online issue, which is available at wileyonlinelibrary.com.]

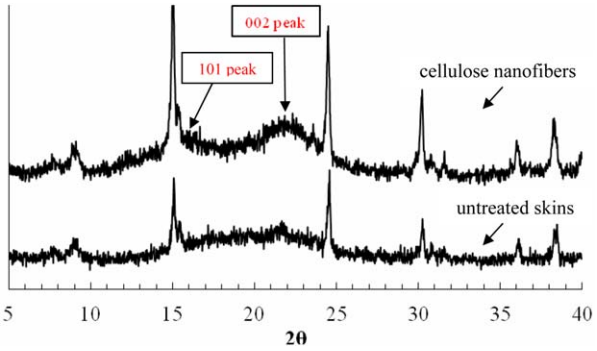

Figure 2. XRD patterns of untreated cactus skins and the isolated cellulose nanofibers. [Color figure can be viewed in the online issue, which is available at wileyonlinelibrary.com.]

However, chemical and physical treatments that were used in the isolation of cellulose nanofibers tend to affect the quality of the cellulose crystallites. Thus, it is necessary to investigate the crystallinity of the produced fibers *via* comparing the XRD patterns of untreated and chemo-mechanically treated samples, which are presented in Figure 2. The XRD patterns show that the peak at around $2\theta = 22°$ is more pronounced, sharper, in case of the cellulose nanofiber powder in comparison with the untreated cactus skins. This is a clear indication of higher crystallinity in the cellulose nanofibers because of the absence of amorphous components such as lignin and pectin. The XRD patterns of both untreated sample and isolated nanofibers show narrow and sharp peaks at around $2\theta = 15.0$, 24.5, 30.2, 36.1, and 38.2°, which are also ascribed to the calcium oxalate crystals of the cactus.[19]

Crystallinity indexes of the untreated cactus skins, CI = 0.31, and cellulose nanofibers, CI = 0.50, were calculated using XRD patterns of Figure 2 and eq. (2). The isolation of nanofibers resulted in a substantial increase in the crystallinity of the samples. However, the crystallinity of the cellulose fibers from cactus skin was still relatively low, which is expected to result in lower rigidity in comparison with cellulose fibers from wood.

Morphological Observations

TEM micrographs of the isolated cellulose nanofibers are presented in Figure 3. A dilute suspension of cellulose nanofibers in water was prepared before the observations. It was observed from the micrographs that almost all of the elements had dimensions, diameters, in the range of 10–50 nm. This suggests that the individual cellulose fibers were effectively separated from the micro-sized fiber bundles during the mechanical treatments and formed a network of nanofibers. The dark spots present in the micrographs, especially in Figure 3(b), are speculated to be the inorganic constituents, such as calcium oxalate crystals, that form the large ash content of the cactus skins, which was shown in Table I.

SEM micrographs of the cryogenically fractured PVA/cellulose nanofiber composites are also shown in Figure 4 to provide insight regarding the level of dispersion of nanofibers in the composites. No signs of fiber agglomerations, in the micron-scale, could be observed in the cross-section of the fractured composites. The surfaces of all composites, even composites with 10% nanofibers, were completely smooth and no fiber pullout was evident on the surfaces. Good dispersion of the fibers suggests that the inclusion of cactus skin cellulose nanofibers can lead to substantial improvements in the mechanical properties of PVA as a result of effective load transfer from matrix to the fibers. The absence of agglomerates also contributes to this enhancement *via* significant reduction in the stress concentrations in the composites.

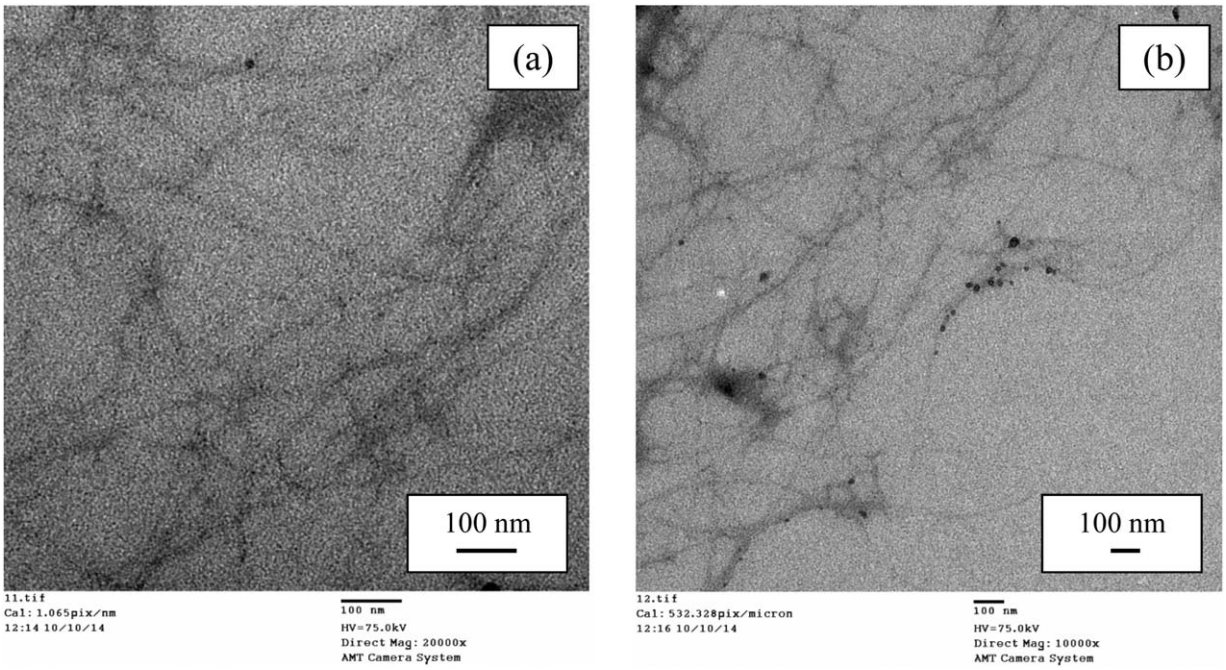

Figure 3. TEM micrographs of the isolated cellulose nanofibers from cactus skins.

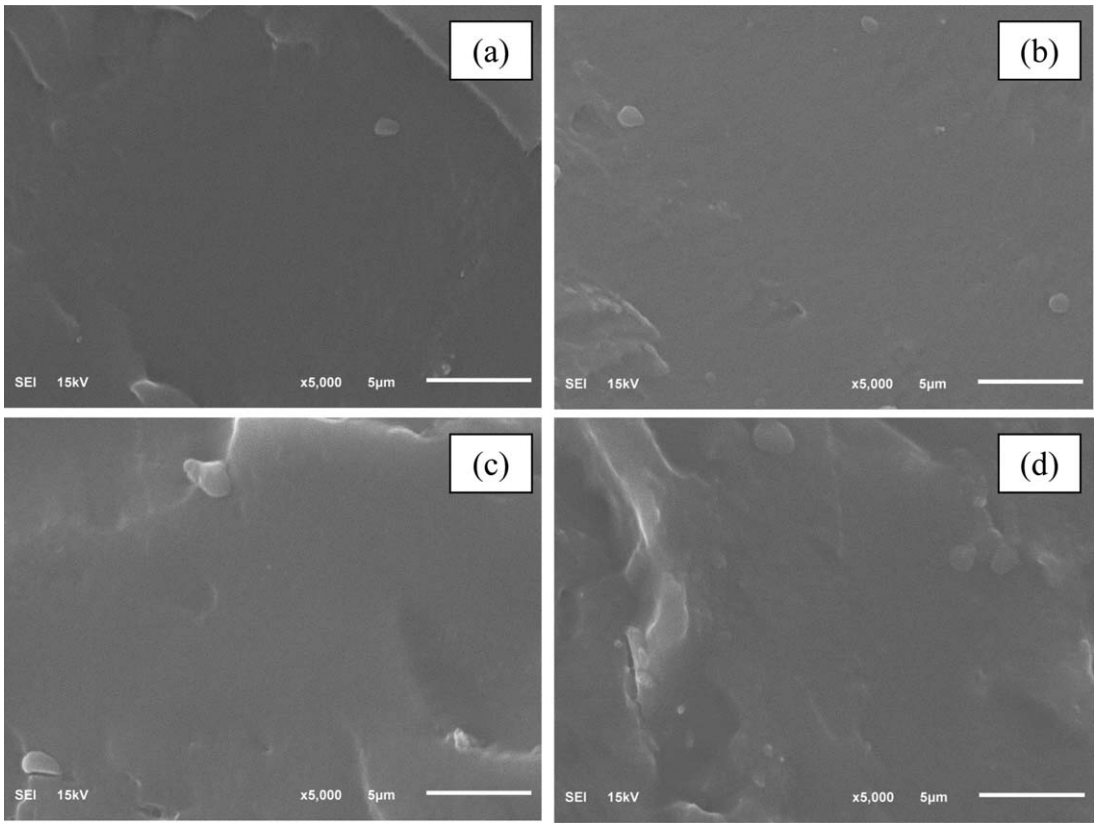

Figure 4. SEM micrographs of the PVA-based composites reinforced with (a) 2%, (b) 5%, (c) 7%, and (d) 10% of cellulose nanofibers from cactus skins with magnification of 5000×.

Tensile Properties

Tensile properties of the prepared nanofibrous film is presented in Table II in comparison with cellulose nanofibers derived from wood based on the data reported in.[17] It is shown in Table II that the tensile modulus and strength of our nanofibrous film was lower than the film made of cellulose nanofibers from wood. This behavior can be ascribed to the relatively low crystallinity of the nanofibers from cactus skins as shown in the XRD, Crystallinity Measurements, and Degree of Polymerization section.

Effects of inclusion of cactus cellulose nanofibers on the tensile properties of PVA matrix are presented in Figures 5–7. Figure 5 shows that the inclusion of even small quantities of the extracted nanofibers resulted in a significant increase in the young's modulus of PVA. Tensile moduli of PVA and PVA/NC(2) were 4.26 and 5.60 GPa, respectively. This behavior is due to the good dispersion of the fibers in the matrix, which was also proven in the morphological observations. Further increase in the concentration of nanofibers up to 10% also improved the modulus of composites, but at a slower rate. Young's modulus of the nanocomposite with 10% cellulose nanofibers was 7.41 GPa, which showed a 74% improvement over pure PVA. The significant improvement in the tensile modulus of the composites can also be ascribed to the creation of a web-like structure in the reinforcements, which was a result of physical entanglements and hydrogen bonding between cellulose nanofibers.[14]

Among all mechanical properties, tensile strength is known to be especially dependent on the level of compatibility between the matrix and reinforcing phase and also to the level of dispersion of fibers.[20] Figure 6 shows the tensile strength of pure PVA in comparison with the produced composites with cellulose nanofibers from cactus skins. It is shown in the figure that, similar to their tensile modulus, the tensile strengths of the composites were also significantly higher than pure PVA. Tensile strengths of nanocomposites with 2 and 10% nanofibers were 30% and 101% higher than that of pure PVA, respectively. Tensile strength of PVA seems to increase linearly with increasing the cellulose nanofiber content.

Figure 7 shows that the inclusion of cellulose nanofibers from cactus skins resulted in a drastic reduction in the deformability of PVA during the tensile tests. Addition of even a small amount of nanofibers, 2%, decreased the elongation at break of PVA from 165 to 7.4%. This is a common phenomenon in composites with

Table II. Tensile Properties of Nanofibrous Films from Cactus Skins and Wood

Source	Tensile Modulus (GPa)	Tensile Strength (MPa)	Elongation at Break (%)
Cactus skins	6.28 ± 0.89	71.2 ± 11.0	7.7 ± 1.0
Wood[17]	7.10 ± 1.79	132.9 ± 9.0	7.1 ± 1.8

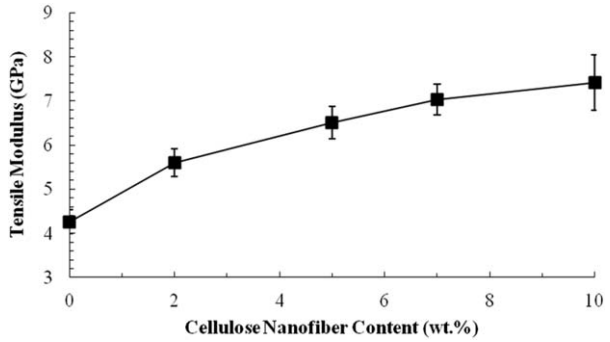

Figure 5. Tensile modulus of PVA and the PVA/nanocellulose composites.

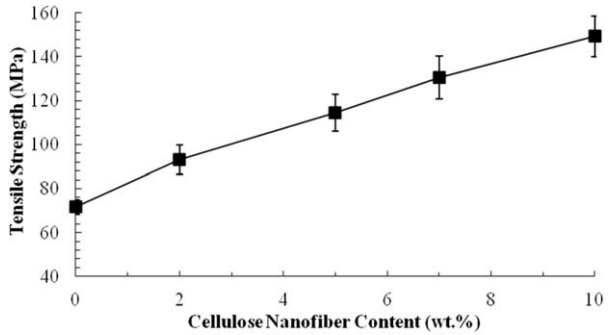

Figure 6. Tensile strength of PVA and the PVA/nanocellulose composites.

different types of reinforcements,[21,22] which can be ascribed to a number of causes. In case of our composites, the cellulose nanofibers have a much lower elongation at break compared with the matrix. As a result, the strong adhesion between the fibers and PVA restricts the deformability of PVA molecules as well.

Thermogravimetric Analysis

Table III and Figure 8 summarize the results of thermogravimetric analysis of untreated cactus skin, isolated cellulose nanofibers, PVA, and PVA/cellulose nanocomposites. In Table III, T_{10} is the temperature for 10% mass loss, whereas $T_{max.dec}$ represents the temperature at which the rate of thermal decomposition of the sample is at its peak. Table III shows that the removal of amorphous constituents, such as lignin and hemicellulose, resulted in an increase in the thermal stability of the cactus skins. T_{10} of untreated skin powder increased from 309.3 to 312.5°C after isolation of the nanofibers. In case of PVA-based composites, three distinct weight loss stages were observed: (i) 100°C because of evaporation of the absorbed moisture in the samples,[23] (ii) 240–340°C caused by dehydration and formation of volatile products,[23] and (iii) 400–460°C because of degradation of the polyene residue, which yields carbon and hydrocarbons.[23] The ash content of cellulose nanofibers, mostly calcium oxalate crystals, is shown to slightly increase the char yield of the composites. Inclusion of the cellulose nanofibers from the cactus skins is also shown to increase the thermal stability of PVA significantly. This can be ascribed to higher thermal stability of cellulose nanofibers and also to the fact that presence of the nanofibers restricts the mobility of matrix molecules.

Table III. TGA Results for Untreated Cactus Skin, Isolated Nanofibers, PVA, and PVA/Cellulose Nanocomposites

Sample	T_{10} (°C)	$T_{max.dec}$ (°C)
Untreated cactus skin	224.7	309.3
Cellulose nanofibers	251.2	312.5
PVA	235.9	252.2
PVA/NC(2)	243.1	269.5
PVA/NC(10)	244.7	295.1

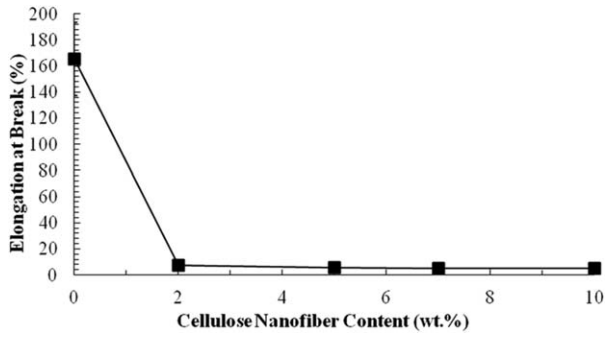

Figure 7. Elongation at breaks of PVA and the PVA/nanocellulose composites.

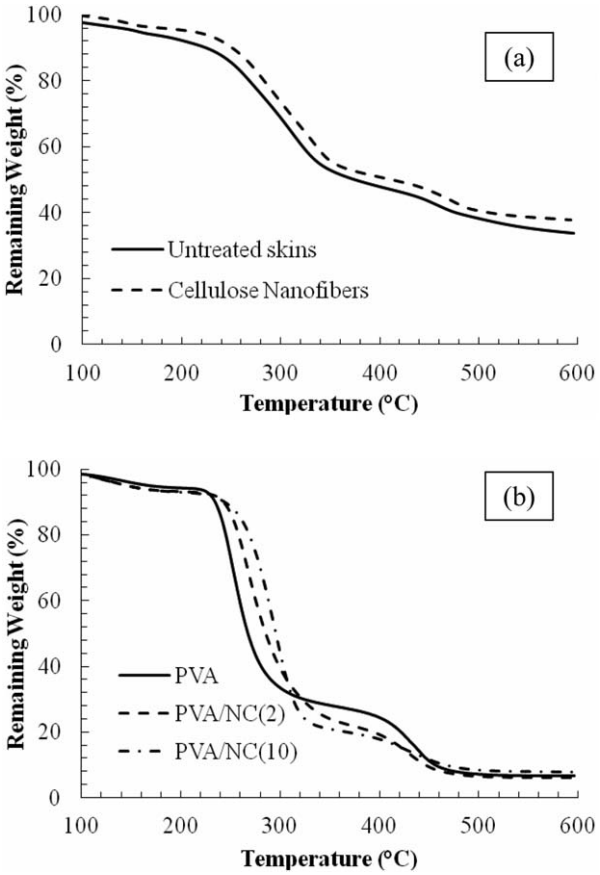

Figure 8. TGA thermograms of (a) untreated skins and isolated cellulose nanofibers and (b) PVA, and PVA/cellulose nanocomposites.

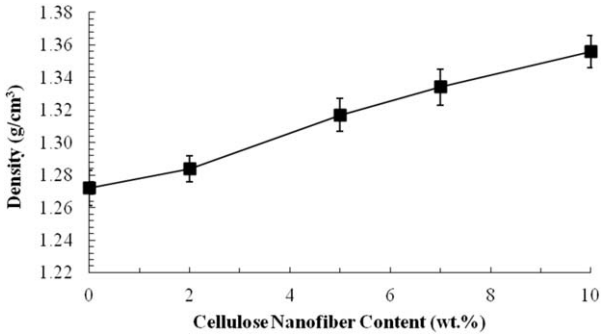

Figure 9. Density of PVA and the PVA/nanocellulose composites.

Density Measurements

Figure 9 shows that the addition of cellulose nanofibers increased the density of PVA because of higher densities of cellulose fibers and calcium oxalate. Density of pure PVA was 1.27 g/cm^3 compared with 1.36 g/cm^3 for PVA/NC(10). Consistent increase in the densities of nanocomposites ensures the absence of significant amounts of air bubbles in the samples, which is in good agreement with morphological observations.

CONCLUSIONS

This work was devoted to the isolation of cellulose nanofibers from the skin of the beavertail cactus, *Opuntia Basilaris*, as a novel and abundant resource for these materials. Composites of polyvinyl alcohol and the extracted cellulose nanofibers were also prepared using solution casting technique. Determination of the chemical composition of the dried cactus skins showed that their cellulose content was relatively high. It was also shown that the skins had a high ash content. FTIR spectroscopy and XRD patterns proved that the isolation of nanofibers was performed successfully. It was also shown in the XRD patterns that the skins had a high content of calcium oxalate crystals. TEM micrographs showed that the isolated nanofibers had diameters in the range of 10–50 nm. Dark spots were also observed that were speculated to be formed by the aforementioned calcium oxalate crystals. SEM micrographs of the cryogenically fractured samples showed that the nanofibers were well dispersed in the PVA matrix. The prepared nanofibrous film was shown to have relatively lower mechanical properties than wood-based cellulose nanofibers from the literature. This was ascribed to the lower crystallinity index of the isolated nanofibers. Tensile characterizations of the composites showed that inclusion of nanofibers increased the modulus and strength of PVA, whereas its deformability decreased significantly. The isolated cellulose nanofibers had higher thermal stability than the untreated skins. Inclusion of nanofibers to PVA was also shown to increase its stability. It was also shown that the inclusion of nanofibers increased the density of PVA.

ACKNOWLEDGMENTS

The authors gratefully acknowledge the financial support from the Natural Sciences and Engineering Research Council of Canada (NSERC).

REFERENCES

1. Habibi, Y.; Mahrouz, M.; Vignon, M. R. *Food Chem.* **2009**, *115*, 423.
2. Wang, B.; Sain, M. *Compos. Sci. Technol.* **2007**, *67*, 2521.
3. El Idrissi, A.; El Barkany, S.; Amhamdi, H.; Maaroufi, A. H. *J. Appl. Polym. Sci.* **2013**, *128*, 537.
4. Taniguchi, T.; Okamura, K. *Polym. Int.* **1998**, *47*, 291.
5. Siró, I.; Plackett, D. *Cellulose* **2010**, *17*, 459.
6. Qua, E. H.; Hornsby, P. R.; Sharma, H. S. S.; Lyons, G.; McCall, R. D. *J. Appl. Polym. Sci.* **2009**, *113*, 2238.
7. Alemdar, A.; Sain, M. *Compos. Sci. Technol.* **2008**, *68*, 557.
8. Jonoobi, M.; Harun, J.; Mathew, A. P.; Oksman, K. *Compos. Sci. Technol.* **2010**, *70*, 1742.
9. Abe, K.; Iwamoto, S.; Yano, H. *Biomacromolecules* **2007**, *8*, 3276.
10. Sreekumar, J.; Sain, M. *Bioresources* **2006**, *1*, 1.
11. Kamphunthong, W.; Hornsby, P.; Sirisinha, K. *J. Appl. Polym. Sci.* **2012**, *125*, 1642.
12. Souza, S. F.; Leao, A. L.; Cai, J. H.; Wu, C.; Sain, M.; Cherian, B. M. *Mol. Cryst. Liq. Cryst.* **2010**, *522*, 42.
13. Lee, S. Y.; Mohan, D. J.; Kang, I. A.; Doh, G. H.; Lee, S.; Han, S. O. *Fibers Polym.* **2009**, *10*, 77.
14. Ramezani Kakroodi, A.; Cheng, S.; Sain, M.; Asiri, A. *J. Nanomater.* to appear. DOI: 10.1155/2014/903498.
15. Szarek, S. R.; Ting, I. P. *Plant Physiol.* **1974**, *54*, 76.
16. Zobel, B. J.; Stonecypher, R.; Browne, C.; Kellison, R. C. *TAPPI* **1966**, *49*, 383.
17. Cheng, S.; Panthapulakkal, S.; Sain, M.; Asiri, A. *J. Appl. Polym. Sci.* **2014**, *131*, DOI: 10.1002/APP.40592.
18. Jonoobi, M.; Harun, J.; Tahir, P. M.; Zaini, L. H.; SaifulAzry, S.; Makinejad, M. K. *Bioresources* **2010**, *5*, 2556.
19. Monje, P. V.; Baran, E. J. *Plant Physiol.* **2002**, *128*, 707.
20. Fu, S. Y.; Feng, X. Q.; Lauke, B.; Mai, Y. W. *Compos. Part B* **2008**, *39*, 933.
21. Ramezani Kakroodi, A.; Rodrigue, D. *J. Appl. Polym. Sci.* **2014**, *131*, DOI: 10.1002/app.40195.
22. Kazemi, Y.; Cloutier, A.; Rodrigue, D. *Compos. Part A* **2013**, *53*, 1.
23. Lu, J.; Wang, T.; Drzal, L. T. *Compos. Part A* **2008**, *39*, 738.